Spectral Reflectance Corrections for Satellite Intercalibrations Using SCIAMACHY Data

David R. Doelling, Constantine Lukashin, Patrick Minnis, Benjamin Scarino, and Daniel Morstad

***Abstract*—High-resolution spectra measured by the ENVISAT SCanning Imaging Absorption spectroMeter for Atmospheric CartograpHY (SCIAMACHY) are used to develop spectral correction factors for satellite imager solar channels to improve the transfer of calibrations from one imager to another. SCIAMACHY spectra averaged for various scene types demonstrate the dependence of reflectance on imager spectral response functions. Pseudo imager radiances were computed separately over land and water from SCIAMACHY pixel spectra taken over two tropical domains. Spectral correction factors were computed from these pseudo imager radiance pairs. Intercalibrations performed using matched 12th Geostationary Operational Environmental Satellite and Terra MODerate-resolution Imaging Spectroradiometer (MODIS) visible ($\sim$0.65 μm) channel data over the same domains yielded ocean and land calibration gain and offset differences of 4.5% and 41%, respectively. Applying the spectral correction factors reduces the gain and offset differences to 0.1% and 3.8%, respectively, for free linear regression. Forcing the regression to use the known offset count reduces the land–ocean radiance differences to 0.3% or less. Similar difference reductions were found for matched MODIS and Meteosat-8 Spinning Enhanced Visible and Infrared Imager channel 2 ($\sim$0.86 μm). The results demonstrate that SCIAMACHY-based spectral corrections can be used to significantly improve the transfer of calibration between any pair of imagers measuring reflected solar radiances under similar viewing and illumination conditions.**

***Index Terms*—Calibrations, satellites, SCanning Imaging Absorption spectroMeter for Atmospheric CartograpHY (SCIAMACHY), spectral response.**

I. Introduction

ACCURATE calibrations of satellite imager channels are essential for converting the observed radiances into physical parameters through remote sensing techniques. The need for these calibrations, particularly acute when monitoring long-term changes in a given variable, has led to the development of the Global Space-based Inter-Calibration System (GSICS) [1]. Operational meteorological satellite imagers have long been equipped with onboard calibration systems for their infrared channels but have typically lacked similar systems for channels measuring spectral reflectance at solar wavelengths. Thus, various methods have been developed to calibrate solar channels against other reference sources, such as well-calibrated aircraft measurements [2], stable desert sites [3], and other satellite imagers [4]. Those approaches have been unsatisfactory because aircraft measurements are sparse and sporadic, the absolute calibrations of the reference surface sites are not well known and can vary, and the accuracies of the reference satellite imagers are highly uncertain. This dilemma has been diminished substantially with the availability of long-lived research satellites having well-calibrated solar channels, employing solar diffusers, particularly the MODerate-resolution Imaging Spectroradiometer (MODIS) [5] on the Terra and Aqua satellites.

Operational geostationary (GEO) and polar-orbiting satellite (POES) imager visible (VIS) and near-infrared (NIR) channels have been calibrated against comparable channels on the MODIS by matching pixels at nadir [6] or off nadir [7] and computing the gain for the target satellite in terms of the MODIS radiances. Thus, the MODIS calibration is transferred to the target imager. Since the channel spectral response functions (SRFs) for a given imager are not the same as their counterparts on other satellites, ideally, the transferred MODIS calibration should be adjusted to account for those spectral differences. To avoid such corrections, only pixels containing cloudy or clear scenes over snow and ocean have been used based on the assumption that such scenes are relatively flat across the relevant wavebands [4], [6], [7]. Theoretical calculations have also been used to develop spectral corrections to improve the accuracy of the calibration transfers [8] but have not yet been verified. High-spectral-resolution satellite measurements have been used to verify onboard calibrations of imager channels by integrating the nearly monochromatic radiances over the imager SRFs and comparing the results to matched radiances observed by the imager [9], [10]. Although this approach, so far, has been used only for calibration adjustment of the coincident imager [9] or the spectrometer [10], presumably, it could be used to develop spectral corrections for transferring infrared calibrations across satellites. High-resolution reflected solar spectra have been measured by the SCanning Imaging Absorption spectroMeter for Atmospheric CartograpHY (SCIAMACHY) on ENVISAT since 2002 [11]. These measurements should be ideal for making empirical spectral corrections to transfer solar-channel calibrations across many different platforms. This letter demonstrates the potential for using SCIAMACHY data to improve the intercalibration of imagers, both past and future.

Manuscript received October 26, 2010; revised March 10, 2011 and June 6, 2011; accepted June 15, 2011. This work was supported in part by the National Aeronautics and Space Administration Earth Science Mission Directorate through the Modeling, Analysis, and Prediction Program and the Clouds and the Earth's Radiant Energy System Project, by the Environmental Sciences Division of the Department of Energy through the Atmospheric Radiation Measurement Program Interagency Agreement under Contract DE-AI02-07ER64546, and by the National Oceanic and Atmospheric Administration Climate Data Records Program through Grant MOA IA1-1016.

D. R. Doelling, C. Lukashin, and P. Minnis are with the Science Directorate, Langley Research Center, National Aeronautics and Space Administration, Hampton, VA 23681-0001 USA (email: David.R.Doelling@nasa.gov; constantine.lukashin-1@nasa.gov; patrick.minnis-1@nasa.gov).

B. Scarino and D. Morstad are with Science Systems and Applications, Inc., Hampton, VA 23666 USA (e-mail: benjiman.r.scarino@nasa.gov).

Digital Object Identifier 10.1109/LGRS.2011.2161751

II. Data and Analysis Methodology

VIS (0.65 μm) channel data taken at a 4-km resolution from the 12th Geostationary Operational Environmental Satellite (GOES-12, G12) during September 2009 were matched with 1-km Terra MODIS channel-1 (0.63 μm) radiances within a domain between 15° N and 15° S and between 55° W and 110° W. A second domain, 15° N to 15° S and 20° E to 20° W, was used to match March 2007 MODIS NIR (0.86 μm) radiances with their counterparts from the 0.81-μm channel on the Meteosat-8 (M8) Spinning Enhanced Visible and Infrared Imager. For each Terra overpass, the data from all pixels for the relevant pair of imagers were averaged over each 0.5° region in the domain. Those 0.5° regional averages containing any saturated MODIS radiances were eliminated. The averaged radiances were then separated between land and water regions, where ocean regions are those having a land percentage less than 10%. All data pairs taken during a one-month period were then used to perform an intercalibration via a nearly simultaneous ray-matching procedure [7].

The regional data pairs were screened to obtain an approximate match in time and viewing angle by only using the data taken within 15 min of each other and with viewing zenith and relative azimuth angles differing by less than 15°. The data taken over water in near-sun-glint conditions were eliminated. The GEO radiances were adjusted to the POES solar zenith angle (SZA) and solar constant E_{S2}. For this study, the subscripts $S1$ and $S2$ correspond to the GEO and POES, respectively. The solar-constant adjustment, i.e., multiplication by E_{S2}/E_{S1}, must be reversed to obtain the absolute values of radiance for a given channel. Since the corrections are based on measured SCIAMACHY solar spectra [12], which may yield slightly different values of E than those associated with each imager channel, any complications due to solar-constant differences are thereby removed. The filtered data are used in a linear regression to obtain gain and offset for one imager in terms of the other

$$L_{S2} = a_i L'_{S1} + b_i \tag{1}$$

where L'_{S1} denotes the radiance of questionable calibration. The G12 radiances are given in terms of 10-b raw digital counts Ct. The coefficients a and b are determined for surface type i. For water and land, $i = 1$ and 2, respectively.

ENVISAT operates in a 98.55°-inclined sun-synchronous orbit crossing the equator around 10:00 LST [11]. Combined measurements from SCIAMACHY channels 1–6 provide continuous high-spectral-resolution radiances at wavelengths from 240 to 1750 nm. This study uses 1-s integration of the SCIAMACHY version 6.03 spectral radiance Level-1 SCI_NL_1P data product [13], yielding a nadir footprint size of about 30 km × 240 km to develop spectral correction factors for the imager channels noted before. The SCIAMACHY spectral radiance and daily solar irradiance [12] are used to derive spectral reflectances over the measured range.

Two data sets are considered: one to illustrate the spectral data and the other to develop correction factors. Average spectral radiances were computed for various scene types using SCIAMACHY data taken from July 2003 through July 2006. The scene types were determined by matching the SCIAMACHY pixels with the Clouds and the Earth's Radiant Energy System Single Scanner Footprint Terra product cloud property data [14] taken approximately half an hour after the ENVISAT overpass. Various constraints were used to specify a uniform scene type. For clear and cloudy scenes, only data having cloud fractions < 0.01 or > 0.99 were used, respectively. Clear ocean and forest data were further restricted to the viewing zenith angles $VZA < 10°$ and to locations equatorward of 50° latitude or $SZA < 45°$, respectively. Deep convective clouds (DCCs) were selected from the tropics for pixels having $VZA < 40°$, $SZA < 45°$, cloud-top temperatures less than 225 K, and optical depths > 70. The radiances and reflectances for a given SRF were computed by convolving them with the scene-type averaged SCIAMACHY spectral radiances and reflectances.

To calculate correction factors for normalizing the calibration of one imager to that of another, SCIAMACHY footprints taken during seasonal months of 2003–2007 in the domains used for matching the GEO and POES data were classified as land or ocean. The spectra from each SCIAMACHY pixel were then convolved with the imager SRFs to compute pseudo imager radiances for each pixel. These pixel radiances presumably cover a large dynamic range in a fairly continuous manner accounting for most cloud and surface types in the domain. They are assumed to represent the radiances in a perfect observing system.

For a given pair of spectral channels, scene, and set of viewing and illumination conditions, the radiance measured by a given imager is related to that of another by the function

$$L_{PS1i} = f_{Si} L_{PS2i} \tag{2}$$

if both are perfectly calibrated. The function f_S is simply the ratio of the two imager radiances, which are the convolved radiances L_P from the SCIAMACHY data. Thus, the actual radiance L_{S1} measured by imager 1 can be obtained from (2) by simply multiplying the value of L_{S2i} from (1) by f_{Si}. Thus, if imagers 1 and 2 are perfectly calibrated, then

$$a_i = 1/f_{Si} \tag{3}$$

if there is no offset radiance for either imager.

III. Results and Discussion

Fig. 1 shows the average SCIAMACHY reflectance spectra for three scene types together with the SRFs for the G12 and Terra MODIS VIS channels [Fig. 1(a)] and the M8 and Terra MODIS NIR channels [Fig. 1(b)]. For clear ocean, the wide G12 band yields a VIS reflectance of 0.0641, which is 3.6% greater than that for MODIS. Because the G12 filter includes the relatively strong reflectance for wavelengths greater than 0.7 μm, this difference rises to 60% over clear forest scenes, where the average G12 reflectance is 0.0836. For the bright DCC scenes, the G12 and MODIS VIS reflectances, 0.8316 and 0.8387, respectively, differ by less than 1%. The differences (not shown) increase to 1.7% for clear snow and 2.7% for stratus clouds and drop nearly to zero for cirrus clouds. Thus, the spectral difference varies nonlinearly with background surface and, hence, intensity.

The two SRFs in Fig. 1(b) barely overlap, yet the NIR reflectance differences are no greater than those for the G12 and

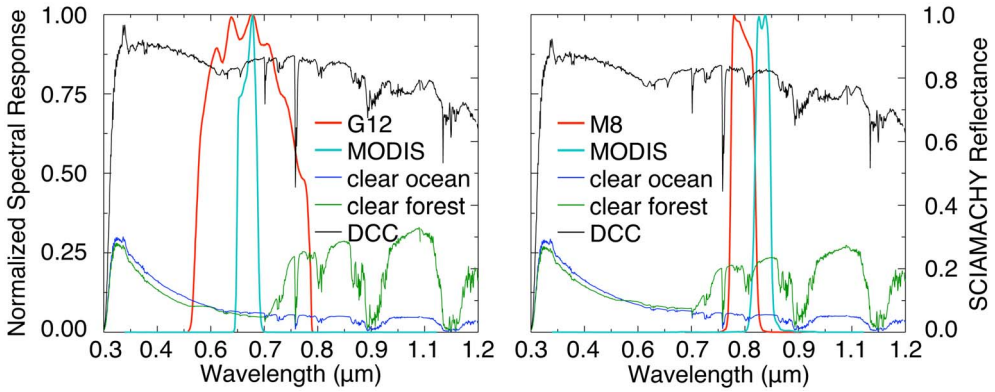

Fig. 1. Average 2003–2006 SCIAMACHY spectra for several scene types overlaid with (a) GOES-12 imager and Terra MODIS channel-1 and (b) Meteosat-8 and Terra MODIS channel-2 SRFs.

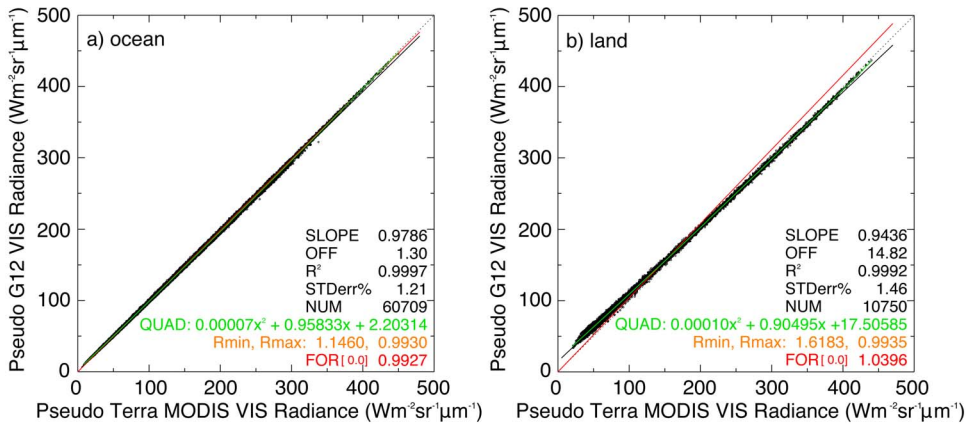

Fig. 2. Scatterplots of pseudo G12 and MODIS VIS radiances determined from SCIAMACHY spectra over G12 tropical domain, autumn 2003–2007. Linear, forced, and quadratic fits are shown in black, red, and green, respectively. The dotted line indicates a slope of unity.

MODIS VIS channels. The SCIAMACHY data indicate that M8 would measure reflectances of 0.0513, 0.1885, and 0.8156, values 5.4%, 14.8%, and 0.5% less than those from MODIS over ocean, land, and DCC clouds, respectively. Differences for the other scene types (not shown) are comparable to those for the VIS channels.

The SCIAMACHY pixel spectra were used to compute pseudo G12 and Terra VIS radiances and M8 and Terra NIR radiances for each season, as described earlier. Those pixel data were used to determine f_S for land and ocean through multiple regression analysis. Results are shown in Figs. 2 and 3, respectively, for the fall VIS and spring NIR pairs. The linear regression slopes for ocean [Fig. 2(a)] and land [Fig. 2(b)] are 0.977 and 0.942, respectively, with corresponding offsets of 1.3 and 14.6 $\mathrm{W \cdot m^{-2} \cdot sr^{-1} \cdot \mu m^{-1}}$. These are qualitatively consistent with the results in Fig. 1(a), particularly at the low end of the range. The regression lines merge toward the line of agreement at the high end of the range corresponding to bright cloudy pixels. However, the linear regression does not satisfactorily fit the data. Quadratic fits (shown in green) match the observations more closely. Linear regressions performed over all seasons reveal a 1.2% range in the slope relative to the annual mean over land. Over ocean, the linear slope varies by 0.8% during the year relative to the annual mean slope. Thus, it is clear that higher accuracy can be obtained using seasonally averaged spectra.

Over water [Fig. 3(a)], the NIR slope and offset are 0.944 and -0.8 $\mathrm{W \cdot m^{-2} \cdot sr^{-1} \cdot \mu m^{-1}}$, respectively, compared to 1.014 and -12.5 $\mathrm{W \cdot m^{-2} \cdot sr^{-1} \cdot \mu m^{-1}}$ for the land scenes [Fig. 3(b)]. The offsets are negative because the MODIS SRF includes the more reflective part of the spectrum. The NIR scatter exceeds that for the VIS channels, most likely because the MODIS SRF does not include the water vapor absorption band near 0.8 μm that can be seen in Fig. 1(b). The standard errors of the NIR linear fits $STDerr$ are two to four times greater than their VIS counterparts in Fig. 2(a). Similar differences in $STDerr$ are found for the quadratic fits. Because saturation tends to clip the range of the MODIS NIR data, the fits are valid only over the observed range of data. To cover the broader range of possible observed radiances, it is assumed that the imager-to-MODIS radiance ratios $Rmin$ and $Rmax$ computed from the fits at the minimum and maximum observed values, respectively, hold for all radiances less than or greater than the respective endpoints. These values are included in Figs. 2 and 3. This assumption could introduce some significant errors if the range is small for the SCIAMACHY data.

Fig. 4 shows the plots of the matched September 2009 G12 and Terra MODIS data along with linear (and forced) regression fits. Slopes for the different types of fits are also listed along with the offset OFF, correlation coefficient R, the standard error of the fits $STDerr$, and the number of samples NUM. The force fits (red) fix the offset at the G12

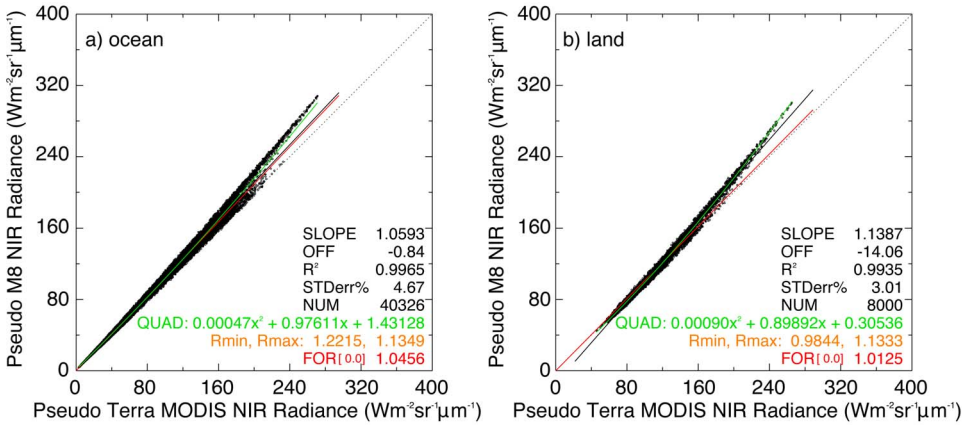

Fig. 3. Same as Fig. 2, except for Meteosat-8 and Terra MODIS channel 2, spring 2003–2007.

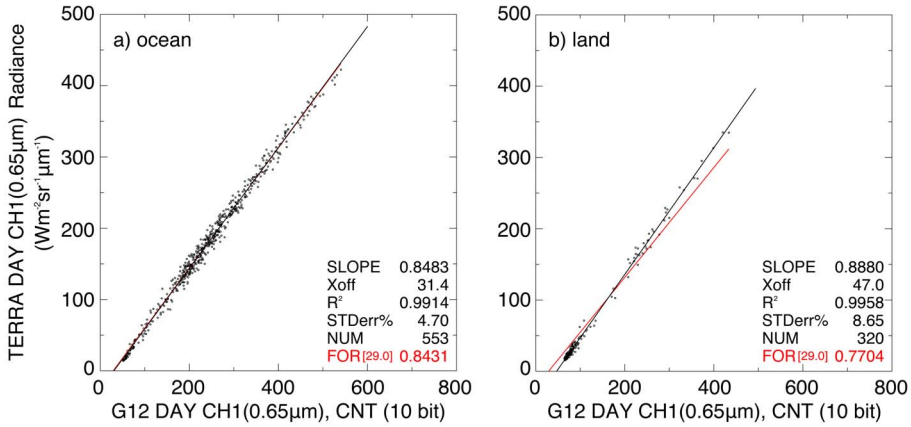

Fig. 4. Scatterplot of matched G12 and Terra MODIS VIS data, September 2009. Linear fits are shown using least squares regression with (black) variable offset and (red) forced offset.

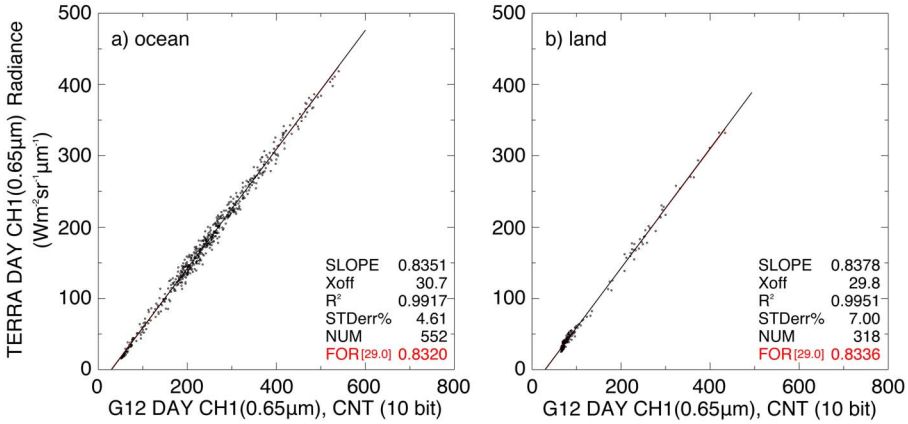

Fig. 5. Same as Fig. 4, except MODIS data adjusted using quadratic fit f_S from Fig. 2.

space count of 29. The ocean least squares fit [Fig. 4(a)] yields an offset of 30.9 Ct, while the land fit [Fig. 4(b)] yields 46.8 Ct. The two least squares slopes differ by 4.5%. For $Ct = 100$, the ocean and land fits yield radiances of 58.9 and 47.3 W $\cdot$ m^{-2} $\cdot$ sr^{-1} $\cdot$ μm^{-1}, respectively. After multiplying the MODIS radiances by the quadratic fits in Fig. 3, the ocean [Fig. 5(a)] and land [Fig. 5(b)] lines are very similar, with differences in the slopes and offsets reduced to $\sim$0.1% and 1.2 Ct, respectively. The linear regressions also appear to fit the data better over the observed dynamic range. For $Ct = 100$, the new ocean and land fits yield radiances of 58.2 and 59.2 W $\cdot$ m^{-2} $\cdot$ sr^{-1} $\cdot$ μm^{-1}, respectively, a difference of 1.7%, down from $\sim$22% for the original fits. The difference for a count of 600 is 0.6 W $\cdot$ m^{-2} $\cdot$ sr^{-1} $\cdot$ μm^{-1} (0.1%), a value reduced from 7.4 W $\cdot$ m^{-2} $\cdot$ sr^{-1} $\cdot$ μm^{-1} (1.5%) for the original fits. The absolute value of the G12 radiances can be obtained

by multiplying the resulting radiances by the ratio of the G12-to-MODIS solar constants.

The slopes of the force fits in Fig. 4 differ by 9.3%. After applying f_S (Fig. 5), the ocean slope increases, while the land slope decreases, reducing the gap to 0.3%. If the adjusted force fits are applied, the ocean–land differences at $Ct = 100$ and 600 are 0.15 (0.2%) and 1.2 $\mathrm{W \cdot m^{-2} \cdot sr^{-1} \cdot \mu m^{-1}}$ (0.3%), reducing the overall reflectance errors compared to the free offset fits.

Similar results (not shown) were found for the fits to the March 2007 M8 and MODIS NIR data. The slopes for the initial fits are 0.475 and 0.514 $\mathrm{W \cdot m^{-2} \cdot sr^{-1} \cdot \mu m^{-1} \cdot Ct^{-1}}$ for land and ocean, respectively. The corresponding offsets are 27.2 and 51.8 Ct. After applying the corrections from Fig. 3, the ocean and land slopes are 0.476 and 0.474 $\mathrm{W \cdot m^{-2} \cdot sr^{-1} \cdot \mu m^{-1} \cdot Ct^{-1}}$, respectively, and the offsets are 50.4 and 50.3 Ct, values very close to the M8 space count of 51. The force fits through that space count yield slopes of 0.479 and 0.477 $\mathrm{W \cdot m^{-2} \cdot sr^{-1} \cdot \mu m^{-1} \cdot Ct^{-1}}$ for land and ocean, respectively. These differences are less than 0.5% compared to 4.2% for the uncorrected force fits. Again, the absolute value of the M8 radiances is obtained by multiplying the resulting radiances by the ratio of the M8 and MODIS solar constants.

IV. Discussion and Conclusion

The differences in ocean and cloud reflectances measured in similar channels on two different imagers are not negligible. The SCIAMACHY spectra reveal that the SRFs give rise to G12 and MODIS VIS reflectance differences ranging from 60% for clear forest to less than 1% over DCC scenes. Somewhat smaller errors were found for the M8 and MODIS NIR channels. SRF corrections should result in the same calibration equations regardless of scene type as long as the variability of the spectral reflectance fields is captured in both the observations used for the spectral response corrections and in the radiances used for the imager intercalibrations. Using two different cases over both water and land, which differ the most spectrally, this letter has demonstrated that the SCIAMACHY spectra can be used to accurately account for the spectral response differences between similar channels, even those that barely overlap, on different imagers yielding calibration equations that differ by less than 0.5%. Based on these initial results, it is concluded that the SCIAMACHY data can be successfully used to develop spectral response corrections for many pairs of imager channels having wavelengths within the SCIAMACHY spectral range. Further study should address the dynamic range, seasonal and regional variabilities, and other issues that impact such corrections and determine how well these initial results represent the accuracy of the corrections in general.

Acknowledgment

This study could not have been completed without the SCIAMACHY data provided by the European Space Agency ENVISAT program. The other satellite data were obtained from the University of Wisconsin Space Science and Engineering Center, Madison, WI. The authors would like to thank J. Burrows, S. Noel, and K. Bramstedt at Bremen University and R. Snel at the Netherlands Institute for Space Research for the assistance with the SCIAMCHY data.

References

[1] M. Goldberg, G. Ohring, J. Butler, C. Cao, R. Datla, D. Doelling, V. Gärtner, T. Hewison, B. Iacovazzi, D. Kim, T. Kurino, J. Lafeuille, P. Minnis, D. Renaut, J. Schmetz, D. Tobin, L. Wang, F. Weng, X. Wu, F. Yu, P. Zhang, and T. Zhu, "The Global Space-based Inter-Calibration System (GSICS)," *Bull. Amer. Meteorol. Soc.*, vol. 92, no. 4, pp. 467–475, Apr. 2011.

[2] P. Abel, B. Guenther, R. N. Gallimore, and J. W. Cooper, "Calibration results for NOAA-11 AVHRR channels 1 and 2 from congruent path aircraft observations," *J. Atmos. Ocean. Technol.*, vol. 10, no. 4, pp. 493–508, Aug. 1993.

[3] C. R. N. Rao and J. Chen, "Post-launch calibration of the visible and near-infrared channels of the advanced very high resolution radiometer on NOAA-14 spacecraft," *Int. J. Remote Sens.*, vol. 17, no. 14, pp. 2743–2747, 1996.

[4] Y. Desormeaux, W. B. Rossow, C. L. Brest, and G. G. Campbell, "Normalization and calibration of geostationary satellite radiances for ISCCP," *J. Atmos. Ocean. Technol.*, vol. 10, pp. 304–325, 1993.

[5] W. L. Barnes, T. S. Pagano, and V. V. Salomonson, "Prelaunch characteristics of the Moderate Resolution Imaging Spectroradiometer (MODIS) on EOS-AM1," *IEEE Trans. Geosci. Remote Sens.*, vol. 36, no. 4, pp. 1088–1100, Jul. 1998.

[6] C. Cao, X. Xiong, A. Wu, and X. Wu, "Assessing the consistency of AVHRR and MODIS L1B reflectance for generating fundamental climate data records," *J. Geophys. Res.*, vol. 113, p. D09 114, May 2008.

[7] P. Minnis, L. Nguyen, D. R. Doelling, D. F. Young, W. F. Miller, and D. P. Kratz, "Rapid calibration of operational and research meteorological satellite imagers, Part I: Evaluation of research satellite visible channels as references," *J. Atmos. Ocean. Technol.*, vol. 19, pp. 1233–1249, 2002.

[8] A. K. Heidinger, C. Cao, and J. T. Sullivan, "Using Moderate Resolution Imaging Spectrometer (MODIS) to calibrate advanced very high resolution radiometer reflectance channels," *J. Geophys. Res.*, vol. 107, no. D23, p. 4702, Dec. 2002.

[9] D. Tobin, H. E. Revercomb, R. O. Knuteson, F. A. Best, W. L. Smith, N. N. Ciganovich, R. G. Dedecker, S. Dutcher, S. D. Ellington, R. K. Garcia, H. B. Howell, D. D. LaPorte, S. A. Mango, T. S. Pagano, J. K. Taylor, P. van Delst, K. H. Vinson, and M. W. Werner, "Radiometric and spectral validation of atmospheric infrared sounder observations with the aircraft-based scanning high-resolution interferometer sounder," *J. Geophys. Res.*, vol. 111, p. D09 S02, Mar. 2006.

[10] A. A. Kokahnovsky, M. Schreier, and W. VonHoyningen-Huene, "The comparison of spectral top-of-atmosphere reflectances measured by AATSR MERIS and SCIAMACHY onboard ENVISAT," *IEEE Trans. Geosci. Remote Sens.*, vol. 5, no. 1, pp. 53–56, Jan. 2008.

[11] H. Bovensmann, J. P. Burrows, M. Buchwitz, J. Frerick, S. Noël, V. V. Rozanov, K. V. Chance, and A. P. H. Goedec, "SCIAMACHY: Mission objectives and measurement modes," *J. Atmos. Sci.*, vol. 56, no. 2, pp. 127–150, Jan. 1999.

[12] J. Skupin, S. Noël, M. W. Wuttke, M. Gottwald, H. Bovensmann, M. Weber, and J. P. Burrows, "SCIAMACHY solar irradiance observation in the spectral range from 240 to 2380 nm," *Adv. Space Res.*, vol. 35, no. 3, pp. 370–375, 2005.

[13] G. Lichtenberg, Q. Kleipool, J. M. Krijger, G. van Soest, R. van Hees, L. G. Tilstra, J. R. Acarreta, I. Aben, B. Ahlers, H. Bovensmann, K. Chance, A. M. S. Gloudemans, R. W. M. Hoogeveen, R. T. N. Jongma, S. Noël, A. Piters, H. Schrijver, C. Schrijvers, C. E. Sioris, J. Skupin, S. Slijkhuis, P. Stammes, and M. Wuttke, "SCIAMACHY Level 1 data: Calibration concept and in-flight calibration," *Atmos. Chem. Phys.*, vol. 6, no. 12, pp. 5347–5367, Nov. 2006.

[14] P. Minnis and S. Sun-Mack, "CERES edition-2 cloud property retrievals using TRMM VIRS and terra and aqua MODIS data, Part I: Algorithms," *IEEE Trans. Geosci. Remote Sens.*, vol. 49, 2011. DOI: 10.1109/TGRS.2011.2144602.